

Marquette University

e-Publications@Marquette

Electrical and Computer Engineering Faculty
Research and Publications

Electrical and Computer Engineering,
Department of

1999


Reduction of Quantum Noise in Transmittance Estimation Using PhotoneCorrelated Beams

Majeed M. Hayat

Adel Joobeur

Bahaa E.A. Saleh

Follow this and additional works at: https://epublications.marquette.edu/electric_fac

 Part of the [Computer Engineering Commons](#), and the [Electrical and Computer Engineering Commons](#)

Marquette University

e-Publications@Marquette

Electrical and Computer Engineering Faculty Research and Publications/College of Engineering

This paper is NOT THE PUBLISHED VERSION; but the author's final, peer-reviewed manuscript. The published version may be accessed by following the link in the citation below.

Journal of the Optical Society of America : A, Vol. 16, No. 2 (1999): 348-358. [DOI](#). This article is © Optical Society of America and permission has been granted for this version to appear in [e-Publications@Marquette](#). Optical Society of America does not grant permission for this article to be further copied/distributed or hosted elsewhere without the express permission from Optical Society of America.

Reduction of Quantum Noise in Transmittance Estimation Using PhotoneCorrelated Beams

Majeed M. Hayat

Center for Electro-Optics, University of Dayton, Dayton,

Adel Joobeur

SVGL, 77 Danbury Road MS450, Wilton, CT

Bahaa E. A. Saleh

Department of Electrical and Computer Engineering, Boston University, Boston, MA

Abstract

The accuracy of optical measurements at low light levels is limited by the quantum noise of the source and by the random nature of the interaction with the measured object. The source noise may be reduced by use of

nonclassical photon-number squeezed light. This paper considers the use of two photon-correlated beams (generated, for example, by spontaneous parametric downconversion) to measure the optical transmittance of an object. The photons of each beam obey a random Poisson process, but are synchronized in time. One beam is used to probe the object while the other is used as a reference providing information on the realization of the random arrival of photons at the object. The additional information available by such measurement may be exploited to improve the accuracy of the measurement. Various estimators, including the maximum likelihood estimator, are considered and their performance is evaluated and compared with the measurement based on single-beam conventional (Poisson) source and maximally squeezed (fixed photon number) source. The performance advantage established in this paper depends on parameters such as the intensity of the source, the transmittance of the object, the quantum efficiency of the detectors, the background noise, and the degree of correlation of the photon numbers in the two beams.

1. Introduction

The accuracy of optical measurements is ultimately limited by the quantum nature of light, which dominates at low light levels when the number of photons per spatial and temporal resolution elements is small.¹⁻⁴ The uncertainty of the measurement is caused by the random fluctuations of the probing optical beam and the random nature of the process of interaction with the probed object. Consider for example the simple process of measuring the transmittance of an object using coherent light as a probe. If we think of each photon of the probe as a particle which is transmitted through the object with a probability equal to the transmittance, then the estimation of the transmittance is akin to estimating the probability of success in a repeated random Bernoulli experiment. However, since the photons themselves arrive at the object at random, in accordance with a Poisson process, an additional uncertainty is introduced. For example, if no photon is received, this could indicate that the photon failed to be transmitted (was absorbed by the object, for example), or that it did not arrive at the object in the first place. In this simple scenario there are two uncertainties: one associated with the random arrival of the photons at the target, and another resulting from the nature of the transmission process—a process of random deletion of photons. Efforts at reducing the noise in the probe beam have fueled an interest in generating amplitude squeezed (sub-Poisson), and quadrature squeezed light, which are forms of non-classical light.⁵⁻⁸

Another source of non-classical light that has generated considerable interest in recent years is photon-correlated beams. Here the light source takes the form of two beams, the photons of each arrive in accordance with a random Poisson process, but the photons of the two beams are, under ideal conditions, perfectly synchronized in time and space. Photon correlated beams can be generated, for example, by spontaneous parametric downconversion.^{9,13} This is a nonlinear process in which each of the photons of a pump interacts with a medium exhibiting the second-order nonlinear effect and creates a pair of photons, a twin, called the signal and idler. Conservation of momentum ensures that if one photon is observed in one direction, its twin must be present in one and only one matching direction. If the pump is in a coherent state, the statistics of the photons in each of the twin beams obeys a Poisson process, but the two processes are, under ideal conditions, completely correlated. Since the joint statistics of the photons of this light source have reduced uncertainty, this light source is squeezed. Photon-correlated beams have been proposed for use in a number of applications including optical communications, cryptography, and tests of the quantum theory of light.¹⁴⁻¹⁹

Photon-correlated beams may be effectively used for optical measurements, for example measurement of the transmittance (or reflectance) of an object. One beam, say the signal, serving as a probe, is transmitting through the object, and both the transmitted signal beam and the idler beam are observed. The information obtained by observing the idler photons provides us with a copy of the realization of the twin signal beam before its transmission through the object. Such information may be used to improve the accuracy of the measurement.

Early work on this problem includes a calculation of the improvement in the accuracy of estimation using an approximation based on the assumption that the mean number of photons collected is large.²⁰ This assumption is not applicable in situations when the illumination is weak. Since the need to enhance the accuracy of measurement beyond the conventional quantum-limited level often arises when the light is weak, there is need to develop a more general theory which establishes the conditions required for achieving an improvement in the estimation accuracy for various estimators of the transmittance, and including realistic non-ideal conditions such as the finite quantum efficiency of the detectors, the background noise, and the partially correlated nature of the twin beams. This is the purpose of the present paper. Although the paper is cast as a theory of estimation of the transmittance (or reflectance) of an object, the results are also applicable to the measurement of quantum efficiency of a detector, and to other radiometric measurement.

This paper is organized as follows. In Section 2 we develop benchmarks for assessing the performance of all the estimates of the transmittance. The mean-square errors associated with the maximum-likelihood estimators are determined for a conventional single-beam setup using a conventional probe with Poisson distributed photons and an ideal probe with deterministic number of photons arriving at the detector in a given time interval. These errors represent the standard single-beam quantum-limited performance and the random- deletion-limited performance, respectively. In Section 3, we consider three estimators based on measurements with photon-correlated beams and determine their associated errors. In Section 4 we examine the effect of various parameters on the performance improvement offered by the photon-correlated-beams measurement relative to the classical single-beam measurement. These parameters include the mean photon flux of the probe beam(s), the level of the transmittance to be estimated, the quantum efficiencies of the detectors used in the measurement, the level of background noise, and the degree of correlation between the photons of the twin beams.

2. Single Beam Measurement

Consider the measurement of the transmittance t of a partially transmitting object by a conventional single-beam setup, as illustrated in Fig. 1. The probe beam carries an average photon flux λ (photons per second), which is reduced to an average photon flux of λ upon transmission through the object. The transmitted beam is detected using a detector with quantum efficiency η operated in the photon counting mode and subjected to background noise equivalent to an average rate of μ photons per second. Such noise results from stray light and free charges that are thermally generated in the detector. The photon countermeasures the number of counts N detected in a time duration T . This number is a random variable with mean value $\eta t \lambda T + \eta \mu T$.

The estimation problem at hand is as follows: Given the measured random variable N , and assuming that the parameters λ , μ , and η are known (from prior accurate measurements of the probe beam and the detector), find an estimate \hat{t} of the transmittance t . This estimate is of course a function of the measurement N , and this dependence will be explicitly denoted by $\hat{t}(N)$ whenever necessary. We also assume knowledge of a probabilistic model for the overall system which is used to determine the probability distribution $P_N(k) = P(N = k)$ of the random variable N , where P stands for probability of an event. A common measure of performance of the estimator is the mean square error defined by

$$\epsilon^2 = E[(\hat{t} - t)^2] = \sum_{k=0}^{\infty} [\hat{t}(k) - t]^2 P_N(k). \quad (1)$$

This error is of course dependent on the chosen estimator \hat{t} and on the probability distribution $P_N(k)$.

The simplest estimator is based on equating the measured random variable N with its expected value, i.e., $N = nt\lambda T + \eta\mu T$, or $\hat{t} = (N - \eta\mu T)/\eta\lambda T$. This estimator is generally not an optimal estimator, and it does not make use of the knowledge of the probability distribution of the measurement N . We shall consider instead the maximum-likelihood (ML) estimator. For a given detected count $N = k$, the ML estimator \hat{t}_{ML} is the value of t that maximizes the probability distribution function of the detected count N evaluated at k . ML estimators are widely used in signal detection and estimation.²¹

To determine the probability distribution $P_N(k)$ we consider the physical model in Fig. 1. Let N_s represent the random number of photons in the probe beam in the counting time T . Upon transmission through the object and detection by the detector, these photons generate a random number of counts N_{ds} in the counter. If N_n is the random number of background counts, then $N = N_{ds} + N_n$. The random number N_{ds} is a deleted version of the random number N_s where every count of N_s survives with probability ηt . The expected values of these random variables are $E(N_s) = \lambda T$, $E(N_{ds}) = \eta t \lambda T$, and $E(N_n) = \eta \mu T$. In order to determine the probability distribution of N , we need to specify the statistics of N_s and N_n . We shall consider two special cases for the statistics of the probe beam photocounts N_s .

1. N_s is a fixed deterministic number (corresponding to maximum photon-number squeezing), and
1. N_s has a Poisson distribution (corresponding to coherent or classical light). In this case $P_{N_s}(k) = P(\eta\lambda k)$, where $P(\delta; k) = \exp(-\delta)\delta^k/k!$ is the Poisson probability distribution function with mean δ .

As for the statistics of the background counts N_n we shall assume that it obeys the Poisson statistics, i.e., $P_{N_n}(k) = P(\eta\lambda T; k)$. Our experience, however, indicates that the exact statistics of the background noise is not critical to cases of interest to us here when the mean value of the background count is low.

A. Probe Beam with Fixed Number of Photons

In ideal antibunched light,⁶ the photon stream is maximally regularized and the number of photons arriving at the detector in any time interval is deterministic. This situation corresponds to light in a maximum photon-number squeezed state. In this case, the probability distribution function of the number of photons arriving at the detector in T units of time in the probe beam is given by

$$P_{N_s}(k) = \delta(k - n), \quad (2)$$

where $\delta(k) = 1$ if $k = 0$, and $\delta(k) = 0$ otherwise. In general, the Mandel parameter,²² which is a measure of uncertainty in the photon count, is defined as

$$Q(0) = \frac{E[(N_s - \bar{N}_s)^2]}{\bar{N}_s} - 1, \quad (3)$$

(where \bar{N}_s is the mean of N_s), and it assumes a minimum value of -1 in the case of maximally photon-number squeezed light. Clearly, uncertainty in transmittance estimation with a direct detection scheme will be at its minimum for this maximally photon-number squeezed state. Each photon is transmitted through the object with probability t . The combined effect of transmission and detection process on the probe beam photons can be thought of as a random deletion process for which the probability that a photon is transmitted and detected is ηt . Thus, the number of detected photons N_{ds} is a binomial random variable (a sum of n independent binary random variables) whose probability distribution function is given by

$$P_{N_{ds}}(k) = B(n, \eta t; k), \quad (4)$$

where

$$B(n, \eta t; k) = \binom{n}{k} (\eta t)^k (1 - \eta t)^{n-k} \quad (5)$$

is a binomial probability distribution function with parameters n and ηt . Using the fact that N_{ds} and N_n are statistically independent, the probability distribution of the detected count N is given by the discrete convolution²³

$$P_N(k) = \sum_{i=0}^{\min(n,k)} B(n, \eta t, i) P(\eta \mu T; k - i). \quad (6)$$

The maximum likelihood estimator $\hat{t}_{F,ML}$, for a given count observation k , is the value of t that maximizes (6). It can be shown that this maximizer is the solution, in the interval $[0,1]$, of the following equation:

$$\frac{d}{dt} P_N(k) = \sum_{i=0}^{\min(n,k)} \left(\frac{i}{t} - \frac{\eta(n-i)}{1-t\eta} \right) \times B(n, t\eta, i) P(\eta \mu T; k - i) = 0. \quad (7)$$

If such a solution does not exist, then $\hat{t}_{F,ML}$ is set to the appropriate end point (zero or one). In Section 4, the above equation is solved numerically to obtain $\hat{t}_{F,ML}$.

The error in the transmittance estimation, $\epsilon_{F,ML}^2$, is evaluated using (1) and (6), and the numerically computed ML estimator $\hat{t}_{F,ML}$ given by (7). This error represents the random-deletion-limited performance in the single-beam case. This error is used hereafter as a benchmark for comparison with results based on photon-correlated beams.

B. Probe Beam with Poissonian Photon Number

In the case of a probe beam with Poissonian photon statistics, the probability distribution function of the number of detected photons N_{ds} is Poissonian with rate $\eta t \lambda$. Furthermore, since the overall count N is an independent sum of two Poisson random variables, it is too a Poisson random variable. The probability distribution function of N is therefore

$$P_N(k) = P(\eta t \lambda T + \eta \mu T; k). \quad (8)$$

(In this case the Mandel parameter $Q(0) = 0$.) By maximizing (8) over t , the maximum likelihood estimator $\hat{t}_{P,ML}$ can be explicitly determined in terms of the number of observed counts N :

$$\hat{t}_{P,ML} = \begin{cases} 0 & \text{if } \frac{N}{\eta \lambda T} \leq \frac{\mu}{\lambda} \\ 1 & \text{if } \frac{N}{\eta \lambda T} \geq 1 + \frac{\mu}{\lambda} \\ \frac{N}{\eta \lambda T} - \frac{\mu}{\lambda} & \text{otherwise} \end{cases} \quad (9)$$

The hard limiting which appears in (9) plays a role only in situations when the photon count is low. The effect of this hard limiting may be neglected otherwise.

The mean-square error $\epsilon_{P,ML}^2$ in this case can be numerically calculated using (9), (8), and (1). When the mean photon count $(\eta t \lambda + \eta \mu)T$ is sufficiently high to warrant neglecting the hard-limiting effect in the expression of $\hat{t}_{P,ML}$, the error $\epsilon_{P,ML}^2$ takes the simple form:

$$\epsilon_{P,ML}^2 = \frac{1}{\eta \lambda T} \left(t + \frac{\mu}{\lambda} \right). \quad (10)$$

In the ideal case when $\mu = 0$ and $\eta = 1$, $\epsilon_{P,ML}^2$ is the error due only to the combined effect of quantum noise and the random deletion of photons. This error is due to noise associated with random deletion, represented by $\epsilon_{F,ML}^2$, and to noise associated with photon-number fluctuation. Since a Poissonian light is the limit in photon fluctuation noise in the semiclassical theory, $\epsilon_{P,ML}^2$ represents the standard quantum limit (SQL) of transmittance estimation noise. By using squeezed light sources, it is possible to reduce the transmittance noise to almost $\epsilon_{F,ML}^2$ which is the lowest error in transmittance estimation using direct detection.

3. Measurement with Photon-Correlated Beams

In this section, we consider the problem of measuring the transmittance of an object using two photon-correlated beams, one used as a probe (signal beam) and the other as a reference (idler beam). The estimation setup is shown schematically in Fig. 2.

The signal beam passes through the partially transmitting object as in the case of the single-beam setup of Section 2. The second beam, the idler, does not go through the object, and is used to provide information on the actual number of photons N_s in the signal beam. After transmission and detection with detection quantum efficiency η_s , N_s is reduced to the detected number of signal photons N_{ds} . The total number of counts in the signal channel, N_{ss} , is the sum of N_{ds} and the additive background noise in the signal channel denoted by N_{ns} . The number of photons from the idler beam, N_i , is in turn reduced after detection in a photon counter with quantum efficiency η_i to N_{di} . The total number of counts in the idler channel, N_{ii} , is the sum of N_{di} and the background noise in the idler channel, N_{ni} . A transmittance estimator \hat{t} , in the photon-correlated light setup, is a function of both N_{ss} and N_{ii} . As in Section 2, we assume that the additive independent background noise photon counts N_{ns} and N_{ni} are Poissonian with means $\eta_s \mu_s T$ and $\eta_i \mu_i T$, respectively.

The statistics of the signal and idler counts are described by the joint probability distribution $P_{N_s N_i}(k, l) = P(N_s = k, N_i = l)$. Under ideal conditions, the signal and idler photons are fully correlated and $P_{N_s N_i}(k, l) = \delta(k - l)P_{N_s}(k)$, where $P_{N_s}(k) = P(N_s = k)$ is the probability distribution function of the number of signal photons. Such conditions are achieved in spontaneous parametric downconversion when the pump is a monochromatic plane wave, the crystal dimensions are infinite, and the signal and idler beams are selected by perfectly matched apertures. In practice, these conditions are not met and the collected signal and idler beams photons are not fully correlated even when matched apertures are used.^{12, 13} Additionally, the transmission of the signal and idler beams through optical elements results in further reduction of the degree of correlation.²⁴

To account for the partial correlation of the signal and idler photon numbers, we adopt a simplified model in which the counts are sums of totally correlated components and totally uncorrelated components: $N_s = N_t + N_{us}$ and $N_i = N_t + N_{ui}$, where N_t is a random number with mean $(1 - \beta)\lambda T$ representing the fully correlated component, and N_{us} and N_{ui} are statistically independent and identically distributed random variables with mean $\beta\lambda T$. This assumption is valid for matched apertures.¹³ The parameter β therefore represents the fraction

of the uncorrelated photons in the signal and idler beams. The case $\beta = 0$ corresponds to full correlation. For simplicity we also use a Poisson model for these random variables so that

$$P_{N_t}(k) = P((1 - \beta)\lambda T; k), \quad (11)$$

and

$$P_{N_{us}}(k) = P_{N_{ui}}(k) = P(\beta\lambda T; k). \quad (12)$$

We now determine the joint probability distribution function of the observed counts $P_{N_{ss}N_{ii}}$. To simplify the derivation, we first note that the uncorrelated signal and idler photons N_{us} and N_{ui} can be combined with the additive background noise N_{ns} and N_{ni} , respectively. Thus, the probability distribution functions of the independent random variables $N_{us} + N_{ns}$ and $N_{ui} + N_{ni}$ are $P(\eta_s t \beta \lambda + \eta_s \mu_s; k)$ and $P(\eta_i \beta \lambda + \eta_i \mu_i; k)$, respectively. Next, we observe that conditioned on the event that the number of twin photons $N_t = n$, the random counts N_{ss} and N_{ii} are independent since the correlation between N_{ss} and N_{ii} is through N_t alone. Hence, by using this conditional independence and an argument similar to the one used in deriving (6), we can write an expression for the conditional joint probability distribution function of N_{ss} and N_{ii} as the product

$$\begin{aligned} & P_{N_{ss}N_{ii}|N_t}(k, l | n) \\ &= \sum_{i=0}^{\min(n, k)} B(n, t\eta_s; i) P(\beta\lambda t \eta_s T + \eta_s \mu_s T; k - i) \\ & \times \sum_{j=0}^{\min(n, l)} B(n, \eta_i; j) P(\beta\lambda \eta_i T + \eta_i \mu_i T; l - j). \quad (13) \end{aligned}$$

The joint probability distribution function $P_{N_{ss}N_{ii}}(k, l)$ can now be obtained by averaging (13) over all possible values of N_t :

$$\begin{aligned} P_{N_{ss}N_{ii}}(k, l) &= \sum_{n=0}^{\infty} P(\beta\lambda T; n) \left[\sum_{i=0}^{\min(n, k)} B(n, t\eta_s; i) \times P(\beta\lambda T \eta_s T + \eta_s \mu_s T; k \right. \\ & \left. - i) \sum_{j=0}^{\min(n, l)} B(n, \eta_i; j) \times P(\beta\lambda \eta_i T + \eta_i \mu_i T; l - j) \right]. \quad (14) \end{aligned}$$

The mean-square error $\epsilon_{\hat{t}}^2$ associated with any photon-correlated estimator \hat{t} can now be evaluated as follows:

$$\epsilon_{\hat{t}}^2 = \sum_{k=0}^{\infty} \sum_{l=0}^{\infty} [\hat{t}(k, l) - t]^2 P_{N_{ss}N_{ii}}(k, l). \quad (15)$$

The estimators considered in this section rely on the positive correlation between the detected signal and idler photons to obtain an estimation error which is below the SQL error level. It is interesting to observe that while

the probability distribution function of the total signal counts N_{ss} is Poissonian, the conditional distribution of N_{ss} given N_{ii} is sub-Poissonian as long as $\beta = 1$. This conditional distribution can be obtained by dividing the joint distribution in (14), by the Poissonian distribution of N_{ii} . To establish a quantitative connection between this conditional sub-Poissonian light and amplitude-squeezed light, we define the conditional Mandel Q -factor (given that $N_t = n$ as:

$$Q^c(n) = \frac{E[(N_{ss} - \bar{N}_{ss})^2 | N_t = n]}{\bar{N}_{ss}} - 1. \quad (16)$$

where \bar{N}_{ss} is the mean of N_{ss} . For the case $\mu_s = \mu_i = 0$ and ideal detection, it can be shown that

$$Q^c(n) = \frac{\beta\lambda T}{n + \beta\lambda T} - 1. \quad (17)$$

The average Mandel Q -factor, \bar{Q} can now be defined by averaging (17) over n . We have numerically evaluated the average Mandel parameter \bar{Q} and the results show that $\bar{Q} = \beta - 1$, which is exactly the fraction of correlated photons in the beams. Hence, if $\beta = 0$, the conditional Mandel parameter is equivalent to that of maximal amplitude squeezing. In contrast, when $\beta = 1$, the conditional Mandel parameter is equal to that of Poissonian light. Thus, a photon-correlated pair of beams resembles a single amplitude squeezed beam in the sense of reducing the uncertainty of the number of photons. This reduction in the average Mandel parameter is manifested in the improved performance of transmittance estimation using photon-correlated beams. The connection between the Mandel parameter and noise in measurement in other applications have been considered in the literature. For example, the dependence of the photocurrent noise in short-pulse direct detection of non-classical light has been investigated by Huttner et al.²⁵ The conditional variance reduction phenomenon has also been investigated in other applications.²⁶

We now develop three estimators and investigate their performance: the maximum likelihood estimator, the count-ratio estimator, and the count-difference estimator.

A. Maximum-Likelihood Estimator

For a given observed signal-channel and idler-channel photon counts $N_{ss} = k$ and $N_{ii} = l$, the ML estimator $\hat{t}_{C,ML}(k, l)$ is obtained by maximizing the joint probability distribution function $P_{N_{ss}N_{ii}}(k, l)$ given in (14). The maximization can be achieved by setting the derivative (with respect to t) of $P_{N_{ss}N_{ii}}(k, l)$ to zero and solving for t . The resulting equation is:

$$\begin{aligned} \sum_{n=0}^{\infty} P(\lambda T; n) & \left\{ \sum_{i=0}^{\min(n,k)} \left[\frac{i}{t} - \frac{\eta_s(n-i)}{1-t\eta_s} - \beta\lambda\eta_s T + \frac{\beta\lambda\eta_s T(k-i)}{\mu_s\eta_s T + \beta\lambda t\mu_s T} \right] \right. \\ & \times B(n, t\eta; i) P(\beta\lambda t\eta T + \eta\mu T; k \\ & \left. - i) \times \sum_{j=0}^{\min(n,l)} B(n, \eta; j) P(\beta\lambda\eta T + \eta\mu T; l-j) = 0. \quad (18) \right. \end{aligned}$$

Equation (18) is solved numerically to obtain $\hat{t}_{C,ML}(k, l)$. When the solution to (18) is not in the interval $[0,1]$, the estimate $\hat{t}_{C,ML}$ is appropriately set to either 0 or 1. Using this expression of the transmittance estimate and the expression of the detected counts joint probability in (14), the estimation error can be numerically evaluated. The results and discussions are deferred to Section 4.

B. Count-Ratio Estimator

This estimator is based on the ratio of counts N_{ss}/N_{ii} , which was first proposed by Jakeman et al.²⁰ The motivation for developing this estimator is the fact that the ratio of the means of N_{ss} and N_{ii} is proportional to $t + \mu_s, \lambda$. The ratio N_{ss}/N_{ii} therefore contains information on the unknown parameter t . The procedure we follow to get the general form of this estimator is to determine the mean $E(N_{ss}/N_{ii})$ and express t in terms of this mean. The ratio estimator, $\hat{t}_{C,R}$ is obtained by replacing $E(N_{ss}/N_{ii})$ in the expression for t by the observed ratio N_{ss}/N_{ii} . We show in the Appendix A that

$$\hat{t}_{C,R}(N_{ss}, N_{ii}) = \frac{1}{\alpha_R} \frac{N_{ss}}{N_{ii}} - \frac{\beta_R}{\alpha_R}, \quad (19)$$

where

$$\alpha_R = \eta_s \lambda T \left\{ \frac{1 - \exp[-\eta_i(\lambda + \mu_i)T]}{(\lambda + \mu_i)T} + (1 + \beta - \eta_i)E[N_{ii}^{-1}u(N_{ii})] \right\}, \quad (20)$$

$$\beta_R = \eta_s \mu_s T E[N_{ii}^{-1}u(N_{ii})], \quad (21)$$

and the function $u(\cdot)$ is the unit-step [$u(x) = 1$, if $x > 0$ and $u(x) = 0$ otherwise]. The derivation of $\hat{t}_{C,R}$ is based on iterated conditional expectations and Bayes; Theorem. The expectation $E[N_{ii}^{-1}u(N_{ii})]$ is computed numerically in Section 4. Values of $\hat{t}_{C,R}$ which are in excess of unity or less than zero are hard limited to unity and zero, respectively. It turns out that as in the case of the ML estimator $\hat{t}_{C,ML}$, the effect of hard limiting is negligible unless the photon counts are very small.

A careful examination of $\hat{t}_{C,R}$ reveals that in the special case when $\eta_i = 1$, $\beta = 0$, and $\mu_s = 0$, no hard limiting is required, and further if $\mu_i = 0$, then $\hat{t}_{C,R}$ is in fact equivalent to the ML estimator $\hat{t}_{C,ML}$. However, the ML estimator does exhibit a performance advantage over the ratio estimator in general as can be seen from the examples of Section 4. The error $\epsilon_{C,R}^2$ associated with $\hat{t}_{C,R}$ can be evaluated numerically using (19) and (14) in (15). The results and discussions are presented in Section 4.

The simplicity of the ratio estimator facilitates deriving an explicit upper bound for the error $\epsilon_{C,R}^2$. This upper bound is then used to determine the asymptotic behavior of $\epsilon_{C,R}^2$ in the limit when λ or T are large. In particular, an asymptotic analysis can be carried out to show that the behavior of $\epsilon_{C,R}^2$ for large values of the intensity λ (assuming $\beta = 0$) is given by:

$$t\{\eta_s^{-1} - \eta_i t[1 - (1 - \eta_i^{-1})^2]\}\lambda^{-1} + o(\lambda^{-1}). \quad (22)$$

The above expression shows that, as expected, $\epsilon_{C,R}^2 \rightarrow 0$ as $\lambda \rightarrow \infty$. The asymptotic expansion in (22) is used in Section 4 to determine the asymptotic advantage of the count-ratio estimator $\hat{t}_{C,R}$ over the Poissonian single-beam estimator $\hat{t}_{P,ML}$.

C. Count-Difference Estimator

We now develop an estimator based on the difference of the photon counts N_{ss} and N_{ii} . The motivation is that in the ideal case of unity quantum efficiency, the difference $N_{ss} - N_{ii}$ represents the number of photons that are not transmitted through the object, and its mean is simply $(1 - t)\lambda$. More importantly, the average effect of background noise can be reduced since N_{ss} and N_{ii} are subtracted from each other. As in the case of the ratio

estimator, to derive the estimator $\hat{t}_{C,D}$, we express $E(N_{ss} - N_{ii})$ in terms of t and then solve for t . The calculations in this case are much simpler and the resulting expression is:

$$\hat{t}_{C,D}(N_{ss}, N_{ii}) = \frac{1}{\alpha_D} (N_{ss} - N_{ii}) - \frac{\beta_D}{\alpha_D}, \quad (23)$$

where

$$\alpha_D = \eta_s \lambda T, \quad (24)$$

$$\beta_D = \eta_s \mu_s T - \eta_i \mu_i T - \eta_i \lambda T. \quad (25)$$

This choice of the coefficients α_D and β_D makes the above estimator unbiased. However, once this estimate is hard-limited to avoid situations when (23) is outside the range $[0,1]$, some bias is introduced. This bias is negligible for reasonably large signal-photon rates. The asymptotic behavior of $\epsilon_{C,R}^2$ for large values of λ can be shown to be

$$\epsilon_{C,D}^2 = \frac{1}{\eta_1 T} \left\{ t[1 - 2\eta_2(1 - \beta)] + \frac{\eta_2}{\eta_1} \right\} \lambda^{-1} + o(\lambda^{-1}), \quad (26)$$

which approaches zero at a rate of $1/\lambda$ as λ increases.

4. Discussion of Results

We have so far considered three situations for the measurement of the transmittance of an object: conventional (Poisson single-beam measurement, maximally squeezed (fixed photon number single-beam measurement, and correlated twin-beam measurement. We have denoted these three cases by the symbols P, F, and C, respectively. We have also examined three types of estimators: maximum likelihood estimators, count-ratio estimator, and count-difference estimator. We have denoted these by the symbols ML, R, and D, respectively. In this section we determine the error ϵ for these situations and estimators. As a relative measure of the performance of a given estimator with respect to the standard quantum-limited performance, we introduce the improvement factor ρ , for each estimator, as the ratio between the estimation error and the error associated with the Poissonian single-beam ML estimator $\hat{t}_{P,ML}$:

$$\rho = \frac{\epsilon}{\epsilon_{P,ML}}. \quad (27)$$

To evaluate ϵ and ρ for each estimator, the probability distributions (6) and (14) are computed numerically. To compute the photon-correlated-beams ML estimator $\hat{t}_{C,ML}$ and the ML estimator using a fixed number of photons $\hat{t}_{F,ML}$, equations (18) and (7) are solved numerically using the joint probability distributions (14) and (6), respectively. To achieve high computational accuracy and speed, and to avoid computer overflow, recursive algorithms (using C programming) were developed to carry out the above computations. For convenience we denote the mean number of signal photons per estimation time λT by n .

A. Asymptotic Performance Advantage

Before presenting the numerical results, we will examine the asymptotic behavior of the improvement factor ρ for the count-ratio estimator $\hat{t}_{C,R}$ and the count-difference estimator $\hat{t}_{C,D}$. Using (22) and (10), we obtain

$$\lim_{n \rightarrow \infty} p_{\hat{t}_{C,R}}^2 = 1 - \eta_s(2 - \eta_i^{-1})t. \quad (28)$$

Similarly, we can use (26) and (10) and obtain

$$\lim_{n \rightarrow \infty} p_{\hat{t}_{C,D}}^2 = \frac{\eta_i}{\eta_s t} + [1 - 2\eta_i(1 - \beta)]. \quad (29)$$

From (28) we deduce that for any η_s , $t > 0$, and $\eta_i > 0.5$, there exists a threshold level n beyond which $p_{\hat{t}_{C,R}}^2 < 1$. This implies that the count-ratio estimator $\hat{t}_{C,R}$ can outperform the Poissonian single-beam ML estimator as long as n and η_i are sufficiently high. Jakeman²⁰ et al. showed that in the absence of background noise photons, a performance advantage is possible if both η_s and η_i are greater than 0.5. Our result therefore guarantees a performance advantage under weaker conditions. On the other hand, (29) indicates that the possible performance advantage associated with the count-difference estimator $\hat{t}_{C,D}$ is very sensitive to the transmittance t . In particular and unlike $\hat{t}_{C,R}$, even under ideal detection conditions ($\eta_s = \eta_i = 1$) and full photon correlation ($\beta = 0$), no performance advantage over the Poissonian single-beam estimator $\hat{t}_{P,ML}$ is predicted when t is very small.

B. Performance Advantage Under Ideal Conditions

We now investigate the performance of the various estimators under the ideal conditions of unit quantum efficiencies, no background photons, and fully photon-correlated beams ($\beta = 0$). Figure 3 (a) shows the error ϵ in the transmittance estimation as a function of the transmittance t , and Fig. 3 (b) shows the dependence of the improvement factor ρ on t . As expected, the fixed-photon-number ML estimator $\hat{t}_{F,ML}$ incurs the smallest absolute estimation error ϵ . This error is the random-deletion-limited error, and it is the best possible performance in transmittance estimation. Confirming the theory presented in Section 3.B, the count-ratio and the ML estimators are identical under these ideal conditions. The error associated with the fixed-photon-number ML estimator $\hat{t}_{F,ML}$, the photon-correlated-beams ML estimator $\hat{t}_{C,ML}$, and the count-ratio estimator $\hat{t}_{C,R}$ are symmetric about $t = 0.5$. This is due to the fact that the uncertainty in these estimators, under the given ideal conditions, is almost exclusively due to the process of photon random deletion (which typically exhibit a variance involving the symmetric term $t(1 - t)$). Specifically, the quantum uncertainty is totally absent in the case $\hat{t}_{F,ML}$, and it is brought to a minimum in the case of $\hat{t}_{C,ML}$ and $\hat{t}_{C,R}$ as a result of the additional information provided by the idler beam. In contrast, the behavior of the Poissonian single-beam ML estimator $\hat{t}_{P,ML}$ does not exhibit any symmetry in the transmittance t . This lack of symmetry is attributed to quantum noise which is strongly signal dependent: the higher t is, the higher number of signal photons which in turn results in a higher absolute variability in the signal photon. This effect results in an increase in the absolute error ϵ . The dip in the curve of $\epsilon_{\hat{t}_{P,ML}}$ near $t = 1$ is a clear indication of the hard-limiting operation involved in the single-beam estimator. The effect of the hard limiting for the single-beam ML estimator becomes noticeable for values of t near unity since there is an increased likelihood of the number of detected photons, N , exceeding $\eta\lambda, T$.

The asymmetric behavior (about $t = 0.5$) of the error associated with the count-difference estimator $\hat{t}_{C,D}$ can be explained in the context of the asymmetry seen in $\epsilon_{\hat{t}_{P,ML}}^2$ and in mind that the mean of $N_{ss} - N_{ii}$ is proportional to $1 - t$ rather than t . The absolute difference between the error associated with the ML fixed-photon-number estimator and any one of the other estimators represents the error due to the quantum fluctuation of the number of source signal photons. Clearly, with the exception of $\hat{t}_{C,D}$, all the photon-correlated-beams estimators exhibit a superior performance in comparison to the conventional single-beam ML estimator $\hat{t}_{P,ML}$ for all values of the parameter t (see Fig. 3 (b)). Furthermore, the improvement factor ρ decreases with t . As for the count-difference estimator, the improvement factor ρ is less than unity as

long as $t > 0.5$. This behavior is predicted by the asymptotic expression (29). The improvement factor ρ is in general a strong function of n and is greatest for the fixed-photon-number estimator $\hat{t}_{F,ML}$ reaching a maximum value of -1.6 dB at $n = 4$ (see Fig. 4). The improvement factor for the photon-correlated-beams estimators $\hat{t}_{C,R}$ and $\hat{t}_{C,ML}$ are approximately -1 dB in the low photon count range ($n < 20$). Furthermore, the performance of $\hat{t}_{C,R}$ and $\hat{t}_{C,ML}$ becomes very comparable to the random-deletion limit as n increases beyond 20. As expected from the asymptotic expression (28), $\rho_{\hat{t}_{C,R}} \rightarrow \sqrt{0.5}$ (-1.5 dB) as $n \rightarrow \infty$. As for the count-difference estimator $\hat{t}_{C,D}$, it starts off with a superior performance to the Poissonian single-beam estimator $\hat{t}_{P,ML}$, but as n increases (approximately beyond 10) its performance approaches that of $\hat{t}_{P,ML}$. This result was also predicted from (29).

C. Effect of Nonideal Detectors and Background Noise

In general, the improvement factors for the correlated-photon-beams estimators ($\hat{t}_{C,D}$, $\hat{t}_{C,ML}$, and $\hat{t}_{C,R}$) and the fixed-photon-number estimator $\hat{t}_{F,ML}$ is reduced as a result of the presence of background noise and low quantum efficiency. Figure 5 shows the dependence of the error E and the improvement factor on the transmittance t for each estimator for the case $n = 20$, $\eta_s = \eta_i = 0.7$, $\mu_s = \mu_i = 5$, and $\beta = 0$. The results indicate that among all the photon-correlated-beams estimators, the ML estimator $\hat{t}_{C,ML}$ has the best performance (as expected). The improvement factor associated with $\hat{t}_{C,ML}$ is as high as -1.5 dB for a transmittance parameter $t = 0.9$. Nonetheless, for low values of the transmittance parameter t (e.g., $t < 0.3$), $\hat{t}_{C,ML}$ shows no improvement over the conventional ML estimator $\hat{t}_{P,ML}$ at such a low signal level n . The fact that $\hat{t}_{C,ML}$ results in a greater error than the conventional single-beam ML estimator $\hat{t}_{P,ML}$ seems counter intuitive at first, since one might suspect that $\hat{t}_{C,ML}$ should always be a better estimator than $\hat{t}_{P,ML}$ since they are based on the same ML principle and the former enjoys the added benefit of the information contained in the idler-channel photons N_{ii} . However, one needs to keep in mind that an ML estimator does not necessarily generate a least mean-square error.²¹ The performance of the count-ratio estimator $\hat{t}_{C,R}$ is slightly inferior to that associated with photon-correlated-beams ML estimator $\hat{t}_{C,ML}$, and the performance of the count-difference estimator $\hat{t}_{C,D}$ is the worst among all estimators (see Fig. 6). No improvement is obtained with the count-difference estimator for any value of n in this case. The improvement factor decreases with n for all the photon-correlated-beams estimators. As n increases beyond 40, approximately, the improvement factor associated with $\hat{t}_{C,R}$ levels off at -0.84 dB which is in agreement with the limit (28).

D. Effect of Partial Correlation of Photons of the Twin Beams

The effect of reduced correlation ($\beta > 0$) between the photon numbers in the signal and idler beams is depicted in Figs. 7 and 8. The performance of each of the photon-correlated-beams estimators is degraded when the value of β is changed from 0 to 0.2. For $n = 20$ and for the set of parameters $\eta_s = \eta_i = 0.7$, $\mu_s = \mu_i = 5$, and $\beta = 0.2$, the photon-correlated-beams ML estimator $\hat{t}_{C,ML}$ remains superior to the Poissonian single-beam estimator for values of the transmittance parameter $t < 0.7$. The count-ratio estimator exhibits a superior performance over the Poissonian single-beam estimator at higher values of n (in excess of 25) as seen in Fig. 8. Hence, both the photon-correlated-beams estimators $\hat{t}_{C,R}$ and $\hat{t}_{C,ML}$ do exhibit a performance advantage over the Poissonian single-beam estimator as long as the signal level n is beyond a certain threshold depending on the parameter β , the background-noise level, and the quantum efficiencies of the detectors.

5. Conclusions

The precision of optical measurement using classical light, under weak illumination conditions, is limited by the quantum noise and the randomness associated with the very process of photon absorption. The effect of quantum noise can be reduced by using non-classical light (sub-Poisson light) or by using a pair of beams exhibiting a positively correlated photon counts. This paper establishes the theory for developing and analyzing estimators of the optical transmittance using a pair of photon-correlated beams generated by parametric

downconversion. We have developed three estimators of the transmittance based on the photon counts from the photon-correlated beams: the maximum likelihood (ML) estimator, the count-ratio estimator, and the count-difference estimator. The average error, which is defined as the square root of the mean-square error, of each of these estimators was compared to the error associated with the Poissonian single-beam ML estimator. As a benchmark for the maximum possible improvement in the estimation performance, the estimators were compared to the ML estimator using maximally photon-number squeezed light (light with a deterministic number of photons) where the estimation error is due only to random deletion of photons.

We have shown that a reduction in the estimation error is possible in comparison to the error associated with the Poissonian single-beam estimator. This improvement in the performance depends on key factors such as the intensity of light, the level of photon correlation, the quantum efficiency of the detectors, the level of background noise, and the actual value of the transmittance. The performance of the count-ratio estimator is generally very similar to that of the ML estimator except when the average photon counts are extremely low (e.g., $n < 5$ for the case when the transmittance t is 0.5). In this low photon-count regime, the ML estimator is superior to all estimators and the performance of the count-difference estimator is comparable to the other two photon-correlated beam estimators. In fact, the errors associated with the photon-correlated ML estimator and the count-ratio estimator approach the ideal-source single-beam limit as the photon count increases. For example, under ideal detection conditions and no background noise, this limit is nearly achieved when the signal photon count is in excess of 20 (assuming $t = 0.5$). In contrast, the performance of the count-difference estimator becomes equivalent to the performance of the Poissonian single-beam estimator when the photon count is high. Therefore, in as much as the count-difference estimator exhibits an improvement in the performance for transmittance values in excess of 0.5, it falls short of the Poissonian single-beam estimator for transmittance values that are less than 0.5. Hence, the count-difference estimator is not always useful in exploiting the photon correlation to reduce quantum noise. Finally, using asymptotic analysis, we have shown that a performance advantage of the count-ratio estimator over the Poissonian single-beam estimator is always possible (under the condition that the quantum efficiency of the idler-channel detector is greater than 0.5) by means of increasing the signal photon counts.

APPENDIX A: DERIVATION OF THE COUNT-RATIO ESTIMATOR

We first start with evaluating the expectation $E(N_{ss}/N_{ii})u(N_{ii})$. By conditioning on N_{ii} , we obtain the conditional mean

$$E \left[\frac{N_{ss}}{N_{ii}} u(N_{ii}) | N_{ii} \right] = N_{ii}^{-1} u(N_{ii}) E(N_{ss} | N_{ii}).$$

Now the last expectation can be computed by first conditioning on N_t , the actual number of twin photons, and then averaging over N_t :

$$E(N_{ss} | N_{ii}) = E[E(N_{ss} | N_{ii}, N_t) | N_{ii}].$$

Now since the correlation between N_{ss} and N_{ii} is through N_t alone, we obtain

$$E(N_{ss} | N_{ii}, N_t) = E(N_{ss} | N_t)$$

and the last conditional mean can be easily evaluated as

$$E(N_{ss} | N_t) = t\eta_s N_t + \eta_s(\mu_s + t\beta\lambda)T.$$

Hence,

$$E(N_{ss}|N_{ii}) = E[E(N_{ss}|N_t)|N_{ii}] = \eta_s(\mu_s + t\beta\lambda)T + t\eta_s E(N_t|N_{ii}),$$

From which we obtain

$$E\left[\frac{N_{ss}}{N_{ii}}u(N_{ii})\right] = \eta_s(\mu_s + t\beta\lambda)TE[N_{ii}^{-1}u(N_{ii})] + t\eta_s E[N_{ii}^{-1}u(N_{ii})E(N_t|N_{ii})].$$

The key step now is to evaluate the conditional expectation $E(N_t|N_{ii})$. From the definition of the conditional mean and Bayes' rule,

$$E(N_t|N_{ii} = \ell) = \sum_{n=0}^{\infty} n \frac{P(N_t = n, N_{ii} = \ell)}{P(N_{ii} = \ell)}.$$

It is convenient to define the random variable M as the sum of the detected background-noise photons N_{ni} and the detected uncorrelated signal photons N_{ui} . Consequently, M is itself Poissonian with mean $n_i(1 - \beta)\lambda T + \eta_i\mu_i T$. Using the law of total probability and the independence of N_t , and M , we obtain

$$\begin{aligned} & \sum_{n=0}^{\infty} n \sum_{i=0}^{\ell} \frac{P(N_t = n, N_{ii} = \ell, M = i)}{P(N_{ii} = \ell)} \\ & \sum_{n=0}^{\infty} n \sum_{i=0}^{\ell} \frac{P(N_{ii} = \ell|N_t = n, M = i)P(N_t = n)P(M = i)}{P(N_{ii} = \ell)}. \end{aligned}$$

Observe that conditional on $M = i$, N_{ii} is simply N_t less a randomly deleted fraction of it (with deletion probability $1 - \eta_i$). Thus,

$$P(N_{ii} = \ell|N_t = n, M = i) = u(n - \ell + 1) \binom{n}{\ell - 1} \eta_i^{\ell-1} (1 - \eta_i)^{n-\ell+i}.$$

We now use the fact that

$$\begin{aligned} P(N_t = n) &= (\beta\lambda)^n \exp(-\beta\lambda)/n!, P(M = i) \\ &= \{\eta_i T[(1 - \beta)\lambda + \mu_i]\}^i \times \exp\{-\eta_i T[(1 - \beta)\lambda + \mu_i]\}/i! \end{aligned}$$

and carry out the algebra to finally obtain

$$E(N_t|N_{ii} = \ell) = (1 - \beta)\lambda \left[(1 - \eta_i)T = \frac{\ell}{\lambda + \mu_i} \right].$$

Using this last result in (A1) we obtain

$$E \frac{N_{SS}}{N_{ii}} u(N_{ii}) = \alpha_R t + \beta_R,$$

where α_R and β_R are given in (20 and (21) respectively.

References

1. B. E. A. Saleh, *Photoelectron Statistics* (Springer, Berlin, 1978).
2. M. Rabbani, "Bayesian filtering of Poisson noise using local statistics," *IEEE Trans. Acoust., Speech, Signal Process.* **36**, 933–937 (1988).
3. R. E. Sequeira, J. A. Gubner, and B. E. A. Saleh, "Quantum-limited image detection," *IEEE Trans. Image Process.* **2**, 18–26 (1993).
4. B. E. A. Saleh, "Quantum noise in optical processing," in *Real-Time Optical Processing*, B. Javidi and J. Horner, eds. (Academic, New York, 1994), pp. 407–437.
5. L. Mandel and E. Wolf, *Optical Coherence and Quantum Optics* (Cambridge U. Press, Cambridge, UK, 1995). Sect. 22.4.
6. M. C. Teich and B. E. A. Saleh, "Photon bunching and antibunching," in *Progress in Optics*, E. Wolf, ed. (North-Holland, Amsterdam, 1988), pp. 1–104.
7. B. E. A. Saleh and M. C. Teich, "Information transmission with photon-number-squeezed light," *Proc. IEEE* **80**, 451–460 (1992).
8. S.-H. Youn, J.-H. Lee, and J.-S. Chang, "Quantummechanical noise characteristics in doubly resonant optical parametric oscillator," *J. Opt. Soc. Am. B* **11**, 2282–2286 (1994).
9. B. R. Mollow, "Photon correlations in the parametric frequency splitting of light," *Phys. Rev. A* **8**, 2684–2694 (1973).
10. C. K. Hong and L. Mandel, "Theory of parametric frequency down conversion of light," *Phys. Rev. A* **31**, 2409–2418 (1985).
11. N. Klyshko, *Photons and Nonlinear Optics* (Gordon & Breach, New York, 1988).
12. A. J. Joobeur, B. E. A. Saleh, and M. C. Teich, "Spatiotemporal coherence properties of entangled light beams generated by parametric down-conversion," *Phys. Rev. A* **50**, 3349–3361 (1994).
13. A. J. Joobeur, B. E. A. Saleh, T. S. Larchuk, and M. C. Teich, "Coherence properties of entangled light beams generated by parametric down-conversion: theory and experiment," *Phys. Rev. A* **53**, 4360–4371 (1996).
14. P. R. Tapster, J. G. Rarity, and J. S. Satchell, "Use of parametric down-conversion to generate sub-Poisson light," *Phys. Rev. A* **37**, 2963–2967 (1988).
15. J. G. Rarity, P. R. Tapster, and E. Jakeman, "Observation of sub-Poisson light in parametric downconversion," *Opt. Commun.* **62**, 201–206 (1987).
16. J. G. Rarity, P. R. Tapster, J. A. Levenson, J. C. Farreau, I. Abram, J. Mertz, T. Debuisschert, A. Heidman, C. Fabre, and E. Giacobino, "Quantum correlated twin beams," *Appl. Phys. B: Photophys. Laser Chem.* **55**, 250–257 (1992).
17. E. A. Perkins, R. J. Carr, and J. G. Rarity, "A twin-beam fibre laser light scattering system," *Meas. Sci. Technol.* **4**, 215–220 (1993).
18. C. K. Hong, S. R. Friberg, and L. Mandel, "Optical communication channel based on coincident photon pairs," *Appl. Opt.* **24**, 3877–3882 (1985).
19. L. Mandel, "Proposal for almost noise-free optical communication under conditions of high background," *J. Opt. Soc. Am. B* **1**, 108–110 (1984).
20. E. Jakeman and J. G. Rarity, "The use of pair production processes to reduce quantum noise in transmission measurement," *Opt. Commun.* **59**, 219–223 (1986).
21. H. V. Poor, *Introduction to Signal Detection and Estimation* (Springer-Verlag, New York, 1988).
22. L. Mandel, "Sub-Poissonian photon statistics in resonance fluorescence," *Opt. Lett.* **4**, 205–207 (1979).
23. H. Stark and J. W. Woods, *Probability, Random Processes, and Estimation Theory for Engineers* (Prentice-Hall, Upper Saddle River, N.J., 1994).

24. B. E. A. Saleh, "Quantum imaging," invited paper presented at the 1997 OSA Annual Meeting, Long Beach, Calif., 1997.
25. B. Huttner, J. J. Baumberg, and J. F. Ryan, "Detection of short pulses of non-classical light," *Opt. Commun.* **90**, 128–132 (1992).
26. J. K. Breslin and G. J. Milburn, "Conditional variance reduction by measurements on correlated field modes," *Phys. Rev. A* **55**, 1430–1436 (1997).

FIGURE CAPTIONS

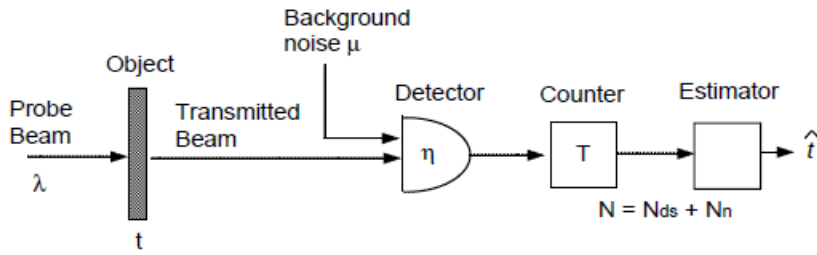


Fig. 1. Schematic diagram of single-beam measurement. A probe beam with photon flux λ is transmitted through an object with transmittance t , and the photon count N (in an interval T) is measured by using a detector (with quantum efficiency η) and a counter. The background-noise photon flux is μ . The measurement N is the sum of the detected probe beam photons N_{ds} and the detected background photons N_n . A single-beam estimator uses the photon count N to generate an estimate \hat{t} of t .

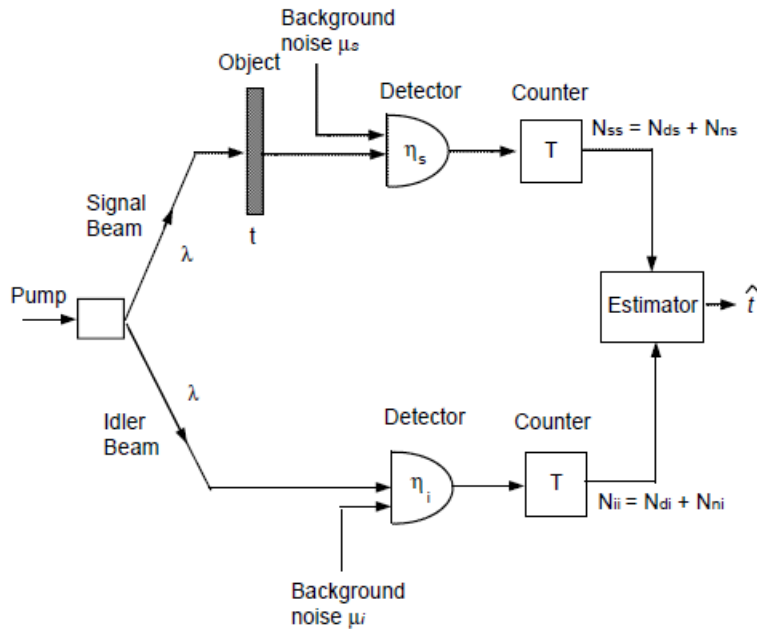


Fig. 2. Schematic diagram of measurement with photon-correlated beams. The signal beam (with photon flux λ) is used as a probe and transmitted through the object (with transmittance t) while the idler beam (also with a photon flux λ) is used as a reference. The observed output N_{ss} of the signal-channel counter is the sum of the detected photons N_{ds} , in the duration T , resulting from the transmitted signal beam and the detected background photons N_{ns} . The observed output N_{ii} of the idler-channel counter is the sum of the detected photons N_{di} resulting from the idler beam and the detected background photons N_{ni} . The quantum

efficiencies of the detectors in the signal and idler channels are η_s and η_i , respectively. A correlated-photon estimator uses the observations N_{s_s} and N_{i_i} to generate an estimate \hat{t} of the transmittance t .

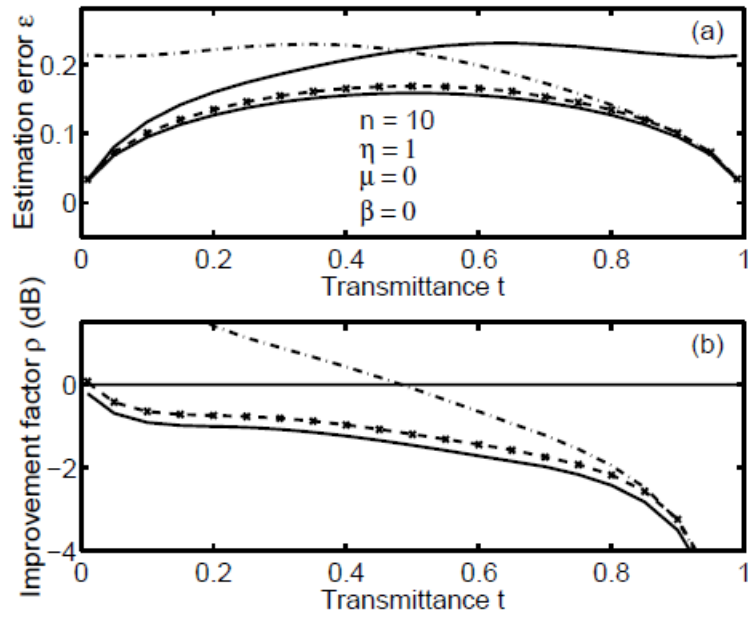


Fig. 3. a) The estimation error ϵ as a function of the transmittance parameter t for the various estimators: Poissonian single-beam ML estimator $\hat{t}_{P,ML}$ (top solid line), fixed-photon-number ML estimator $\hat{t}_{F,ML}$ (bottom solid line), photon-correlated-beams ML estimator $\hat{t}_{C,ML}$ (dashed line), count-ratio estimator $\hat{t}_{C,R}$ (represented by the symbol \times and overlaying the dashed line), and count-difference estimator $\hat{t}_{C,D}$ (dashed/dotted line appearing near the top portion of the figure). The estimation parameters are: $n = 0$, $\eta_s = \eta_i = 1.0$, $\mu_s = \mu_i = 0$, and $\beta = 0$. Notice the complete overlap between the count-ratio estimator curve and the photon-correlated-beams ML estimator curve. b) The improvement factor ρ as a function of the transmittance parameter t .

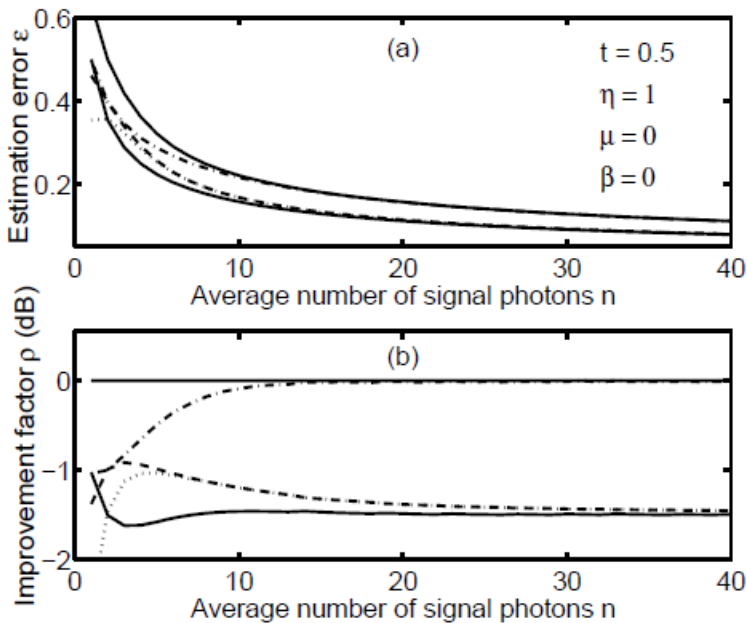


Fig. 4. a) The estimation error ϵ as a function of the mean number of signal photons n for the various estimators: Poissonian single-beam ML estimator $\hat{t}_{P,ML}$ (top solid line), fixed-photon-number ML estimator $\hat{t}_{F,ML}$ (bottom solid line), photon-correlated-beams ML estimator $\hat{t}_{C,ML}$ (dashed line just above the bottom solid line), count-ratio estimator $\hat{t}_{C,R}$ (dotted line), and count-difference estimator $\hat{t}_{C,D}$ (dashed/dotted line). The estimation parameters are: $t = 0.5, \eta_s = \eta_i = 1.0, \mu_s = \mu_i = 0$, and $\beta = 0$. Notice the complete overlap between the count-ratio estimator curve and the photon-correlated-beams ML estimator curve. b) The improvement factor ρ as a function of the mean number of signal photons n .

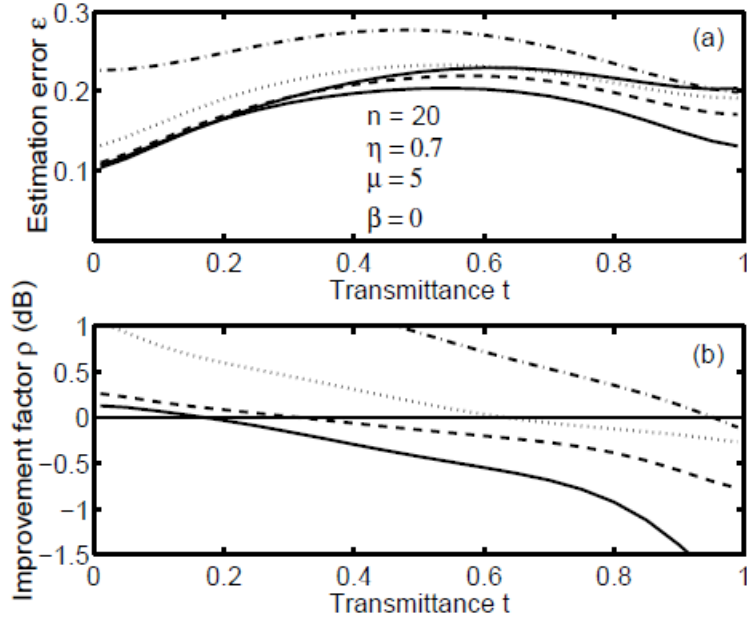


Fig. 5. a) The estimation error ϵ as a function of the transmittance parameter t for the various estimators: Poissonian single-beam ML estimator $\hat{t}_{P,ML}$ (top solid line), fixed-photon-number ML estimator $\hat{t}_{F,ML}$ (bottom solid line), photon-correlated-beams ML estimator $\hat{t}_{C,ML}$ (dashed line), count-ratio estimator $\hat{t}_{C,R}$ (dotted line), and count-difference estimator $\hat{t}_{C,D}$ (dashed/dotted line). The estimation parameters are: $n = 20, \eta_s = \eta_i = 0.7, \mu_s = \mu_i = 5$, and $\beta = 0$. b) The improvement factor ρ as a function of the transmittance parameter t .

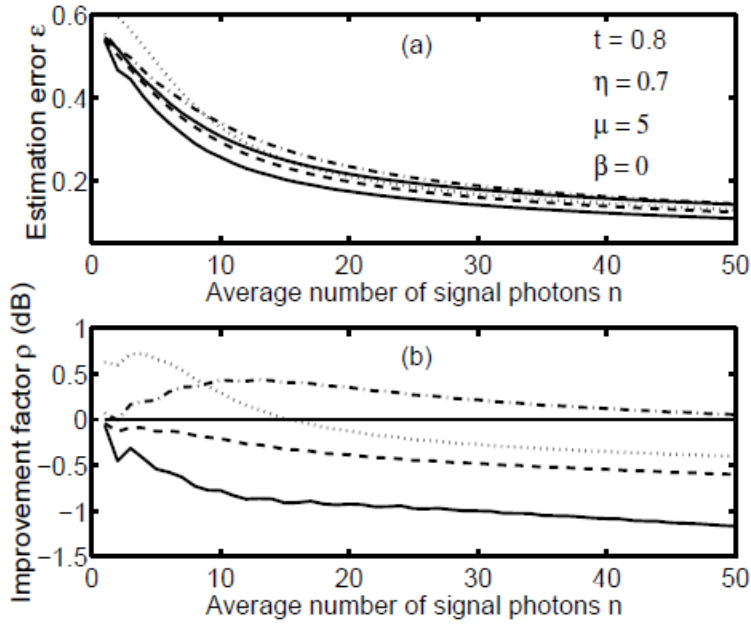


Fig. 6. a) The estimation error ε as a function of the mean number of signal photons n for the various estimators: Poissonian single-beam ML estimator $\hat{t}_{P,ML}$ (top solid line), fixed-photon-number ML estimator $\hat{t}_{F,ML}$ (bottom solid line), photon-correlated-beams ML estimator $\hat{t}_{C,ML}$ (dashed line), count-ratio estimator $\hat{t}_{C,R}$ (dotted line), and count-difference estimator $\hat{t}_{C,D}$ (dashed/dotted line). The estimation parameters are: $T = 1$, $t = 0.8$,

$\eta_s = \eta_i = 0.7$, $\mu_s = \mu_i = 5$, and $\beta = 0$. b) The improvement factor ρ as a function of the mean number of signal photons n .

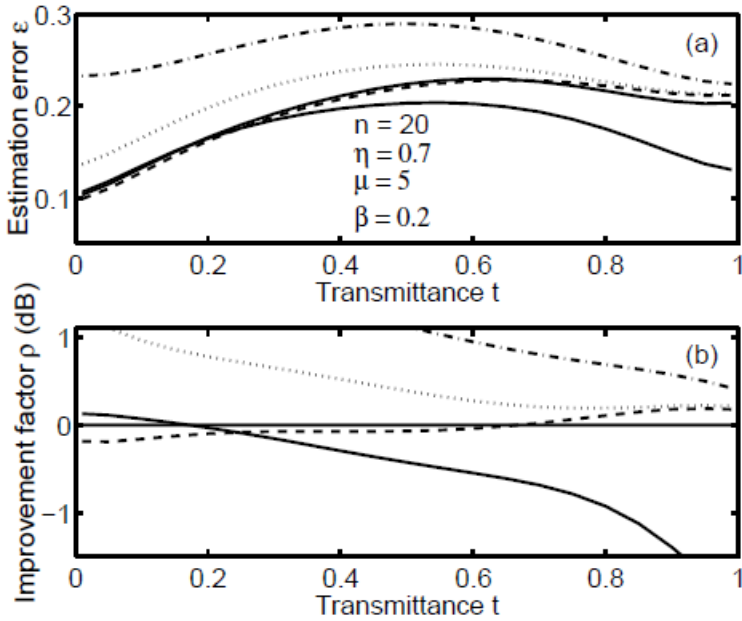


Fig. 7. a) The estimation error ε as a function of the transmittance parameter t for the various estimators: Poissonian single-beam ML estimator $\hat{t}_{P,ML}$ (top solid line), fixed-photon-number ML estimator $\hat{t}_{F,ML}$ (bottom solid line), photon-correlated-beams ML estimator $\hat{t}_{C,ML}$ (dashed line), count-ratio estimator $\hat{t}_{C,R}$ (dotted line),

and count-difference estimator $\hat{t}_{C,D}$ (dashed/dotted line). The estimation parameters are: $T = 1$, $n = 20$, $\eta_s = \eta_i = 0.7$, $\mu_s = \mu_i = 5$, and $\beta = 0.2$. b) The improvement factor ρ as a function of the transmittance parameter t .

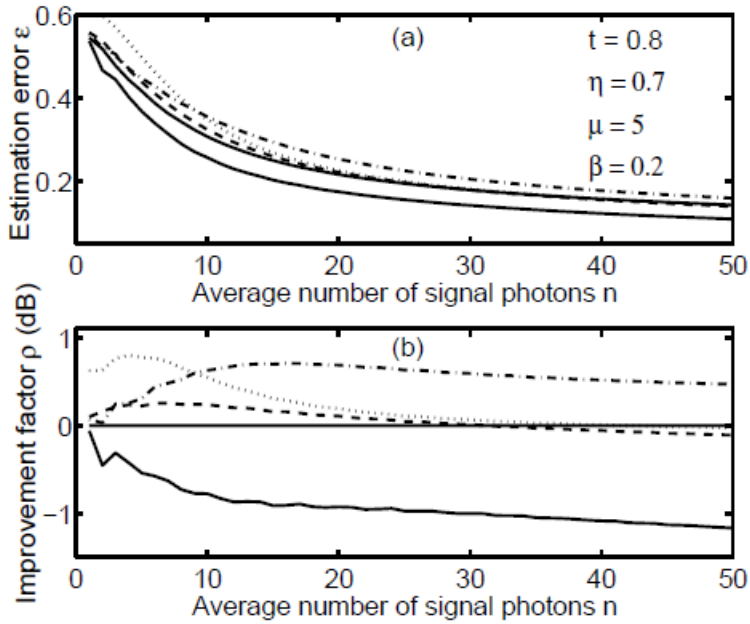


Fig. 8. a) The estimation error ϵ as a function of the mean number of signal photons n for the various estimators: Poissonian single-beam ML estimator $\hat{t}_{P,ML}$ (top solid line), fixed-photon-number ML estimator $\hat{t}_{F,ML}$ (bottom solid line), photon-correlated-beams ML estimator $\hat{t}_{C,ML}$ (dashed line), count-ratio estimator $\hat{t}_{C,R}$ (dotted line), and count-difference estimator $\hat{t}_{C,D}$ (dashed/dotted line). The estimation parameters are: $T = 1$, $t = 0.8$, $\eta_s = \eta_i = 0.7$, $\mu_s = \mu_i = 5$, and $\beta = 0.2$. b) The improvement factor ρ as a function of the mean number of signal photons n as a function of the mean number of signal photons n .